NASA TECHNICAL MEMORANDUM

NASA TM X-1559

NASA TM X-1559

EXPERIMENTAL EVALUATION OF SEVERAL ADVANCED ABLATIVE MATERIALS AS NOZZLE SECTIONS OF A STORABLE-PROPELLANT ROCKET ENGINE

by A. J. Pavli

Lewis Research Center

Cleveland, Ohio

NATIONAL AERONAUTICS AND SPACE ADMINISTRATION • WASHINGTON, D. C. • APRIL 1968

NASA TM X-1559

EXPERIMENTAL EVALUATION OF SEVERAL ADVANCED ABLATIVE MATERIALS AS NOZZLE SECTIONS OF A STORABLE-PROPELLANT ROCKET ENGINE

By A. J. Pavli

Lewis Research Center
Cleveland, Ohio

NATIONAL AERONAUTICS AND SPACE ADMINISTRATION

For sale by the Clearinghouse for Federal Scientific and Technical Information
Springfield, Virginia 22151 – CFSTI price $3.00

EXPERIMENTAL EVALUATION OF SEVERAL ADVANCED ABLATIVE MATERIALS AS NOZZLE SECTIONS OF A STORABLE-PROPELLANT ROCKET ENGINE

by A. J. Pavli

Lewis Research Center

SUMMARY

Eighteen ablative materials were evaluated for their relative erosion resistance in test firings of 22 nozzles in a storable-propellant engine of a 1.2-inch (3.05-cm) diameter throat at a chamber pressure of 100 psia (689.5 kN/m^2). The materials investigated were the phenolic, polyimide, phenolic plus polyamide, epoxy novalac, and phenylsilane resins, reinforced with silica, quartz, and carbon-silica fibers. Quartz reinforcement was superior to silica with the three resins tested. The lower erosion rate is attributed to the higher melting temperature of quartz. Carbon-silica reinforcement exhibited the highest erosion rate. Its relatively poor performance is attributed to the rapid oxidation of the carbon. Ablatives made of phenolic resin had lower erosion rates than all other resins tested.

Erosion at mixture ratios of 1.6 was greater than at mixture ratios of 2.0. Nozzle convergent entrance angle, throat radius of curvature, and source or resin supplier had no apparent effect on erosion resistance. A slight effect of fabrication technique on erosion was detected.

INTRODUCTION

Previous testing of ablative materials as nozzle sections of a storable-propellant (nitrogen tetroxide and a 50-50 percent blend of unsymmetrical dimethylhydrazine with anhydrous hydrazine) rocket engine has screened many candidate materials and revealed the general classes of materials that look most promising in this environment (ref. 1). Reported herein are the results of further investigation into the more promising of these materials. The investigation was conducted to determine optimum resins, reinforce-

ments, and combinations and to study the effects of other material and geometry variables on throat erosion resistance. Effects of propellant mixture ratio and material fabrication techniques were also examined briefly. Eighteen nozzle materials were evaluated. These materials included phenolic, polyimide, phenolic plus polyamide, epoxy novalac, and phenyl-silane resins, reinforced with silica, quartz, and carbon-silica fibers. The nozzles were of 1.2-inch (3.05-cm) throat diameter, were run at a constant chamber pressure of 100 psia (689.5 kN/m^2), and nominally yielded 140 pounds thrust (622 N).

APPARATUS

The tests were performed in a small vertical firing rocket facility shown in figure 1. The engine was mounted to fire down into a water jacketed pipe which ducted the exhaust products into a water spray scrubber and then to an atmosphere vent (fig. 2). The propellants were supplied to the engine from pressurized propellant tanks through hydraulic valves that were controlled by a closed loop servocontroller. The oxidant valve was

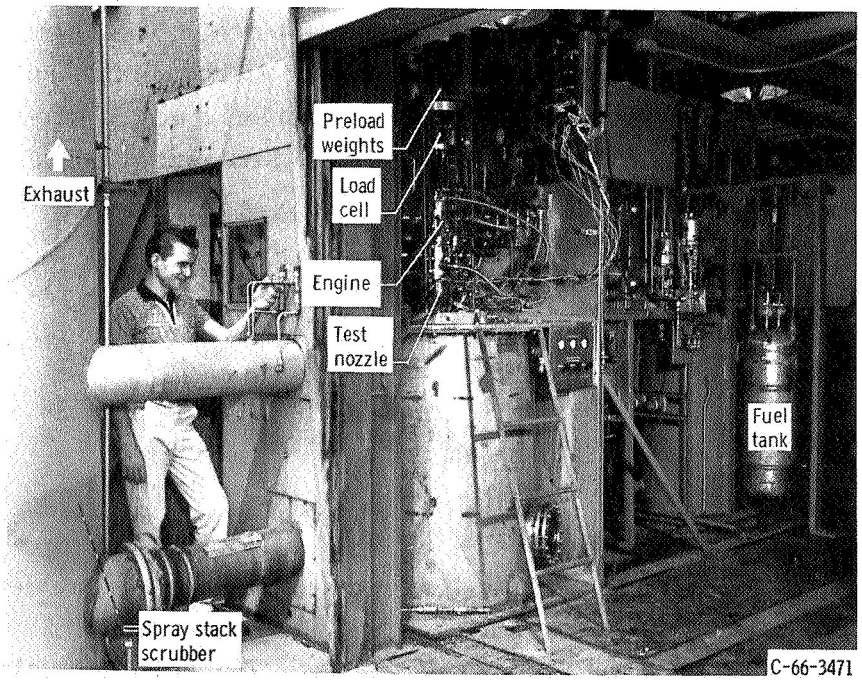

Figure 1. - Photograph of test installation.

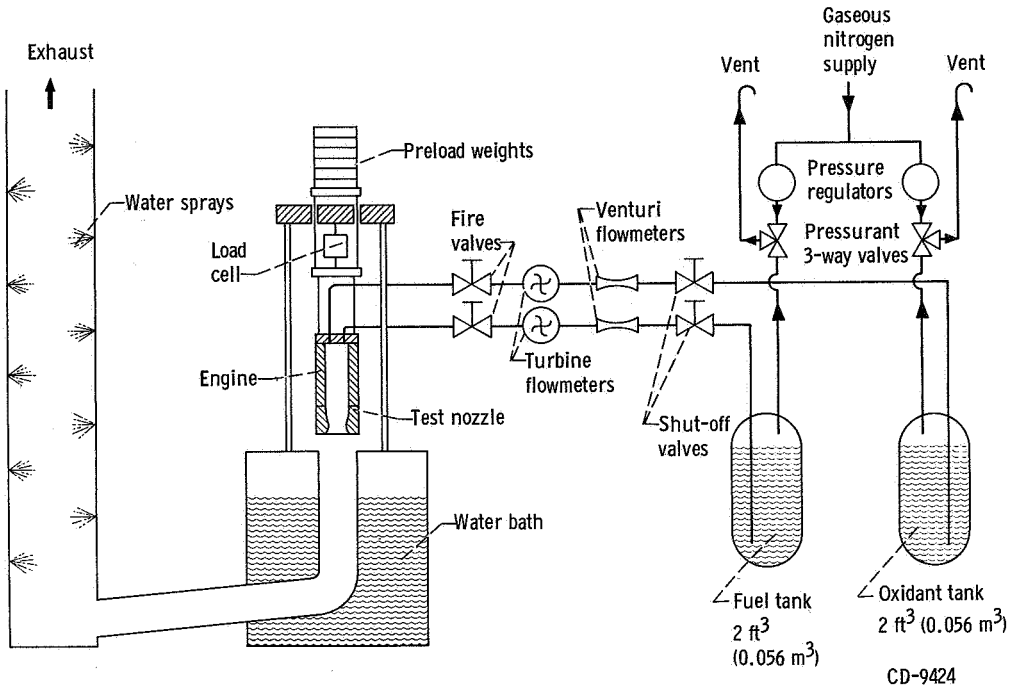

Figure 2. - Test installation.

automatically modulated to maintain a constant chamber pressure of 100 psia (689.5 kN/m^2). The fuel valve was automatically modulated to maintain a constant oxidant-fuel mixture ratio of either 1.6 or 2.0. As the throat of the ablative nozzles eroded, the propellant flows were automatically increased to maintain the preset chamber pressure and O/F values.

The thrust chamber (fig. 3) was composed of three 2.875-inch (7.30-cm) diameter, water-cooled spool sections bolted together. A 2.31-inch (5.87-cm) diameter injector was bolted to the head end of the chamber via a water-cooled transition ring. The nozzle was attached to the other end of the chamber with a transition ring when necessary. (Nozzle inlets of 2.94-in. (7.47-cm) diameter did not need a transition ring.) The length of the chamber from injector to throat was approximately 14.1 inch (35.8 cm) with a nominal characteristic length L* of 65 inches (165 cm).

The injector was a 10-element triplet with two oxidant streams impinging on each fuel stream one inch (2.54 cm) from the injector face (see fig. 4). Combustion-chamber pressure communicated with the injector P_c tap through a notch cut into the transition ring as shown.

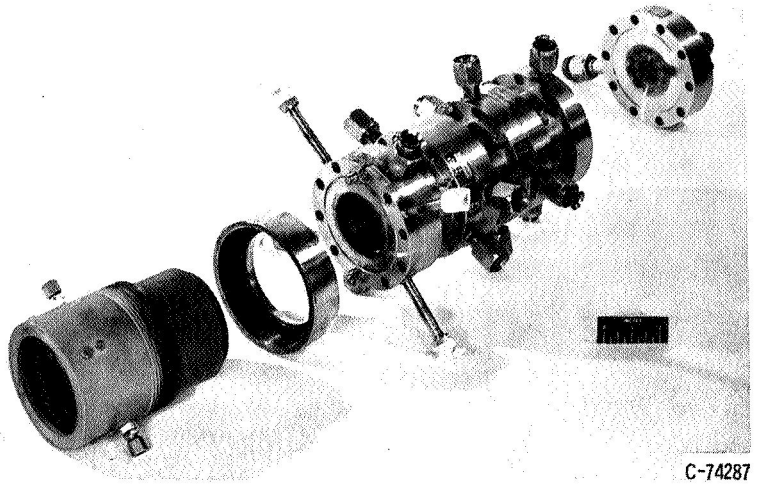

C-74287

(a) Disassembled.

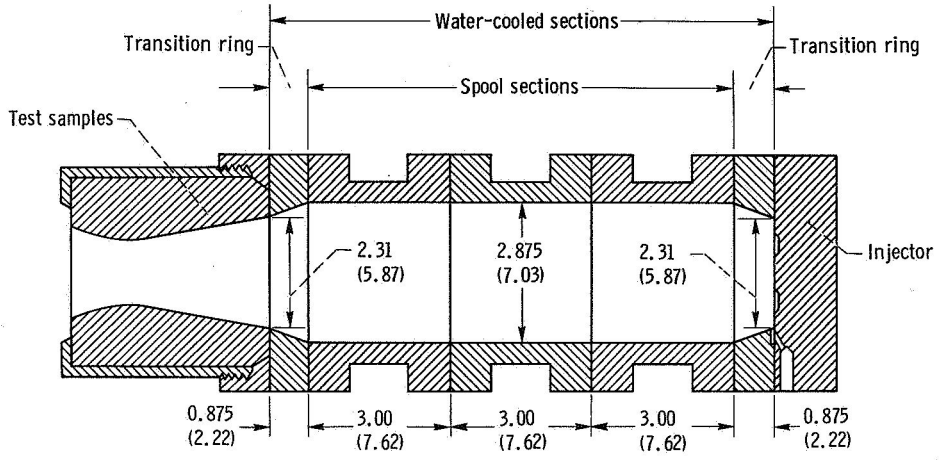

(b) Assembled.

CD-8310

Figure 3. - Engine configuration. (All linear dimensions are in inches (cm)

Test nozzles were fabricated into four different configurations. These are shown in figure 5. Configuration 1 (fig. 5(a)) has an 11^{o} convergence half angle from the 2.35-inch (5.97-cm) diameter inlet to the throat, with a 3.5 inch (8.89 cm) throat radius of curvature. A transition ring was required to mate it to the 2.875-inch (7.30-cm) chamber diameter. Configuration 2 has a 17^{o} convergence half angle (see fig. 5(b)) from a 2.94-inch (7.47-cm) diameter inlet to the throat, and required no transition ring from the chamber to the nozzle. Configuration 3 has the steepest convergence half angle of all configurations, 25^{o}. The radius of curvature at the throat was 1.0 inches (2.54 cm), the smallest of the configurations tested. Configuration 4 was identical to configuration 3

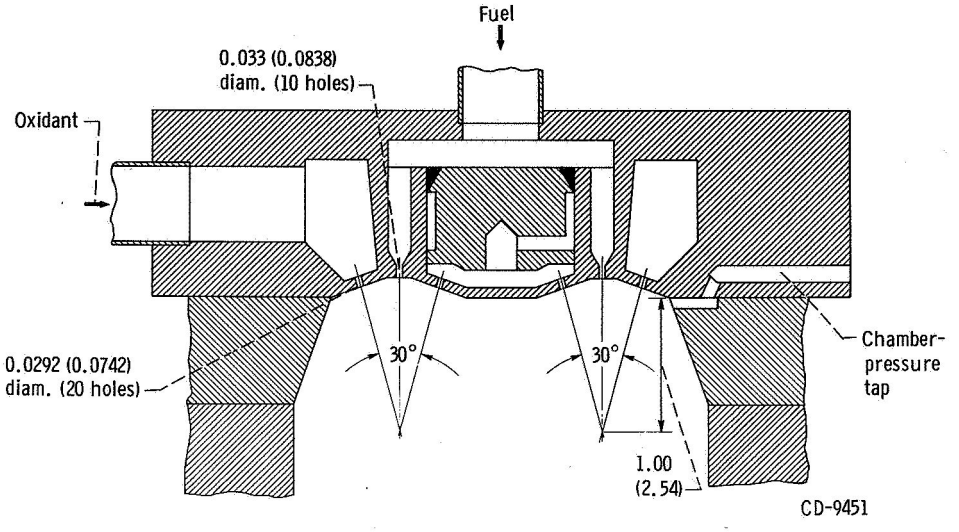

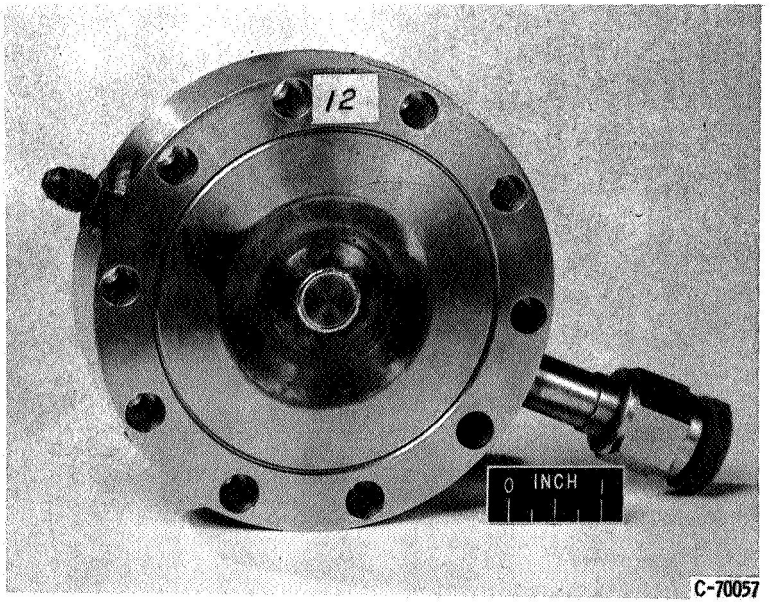

Figure 4. - Injector configuration. (All linear dimensions are in inches (cm)).

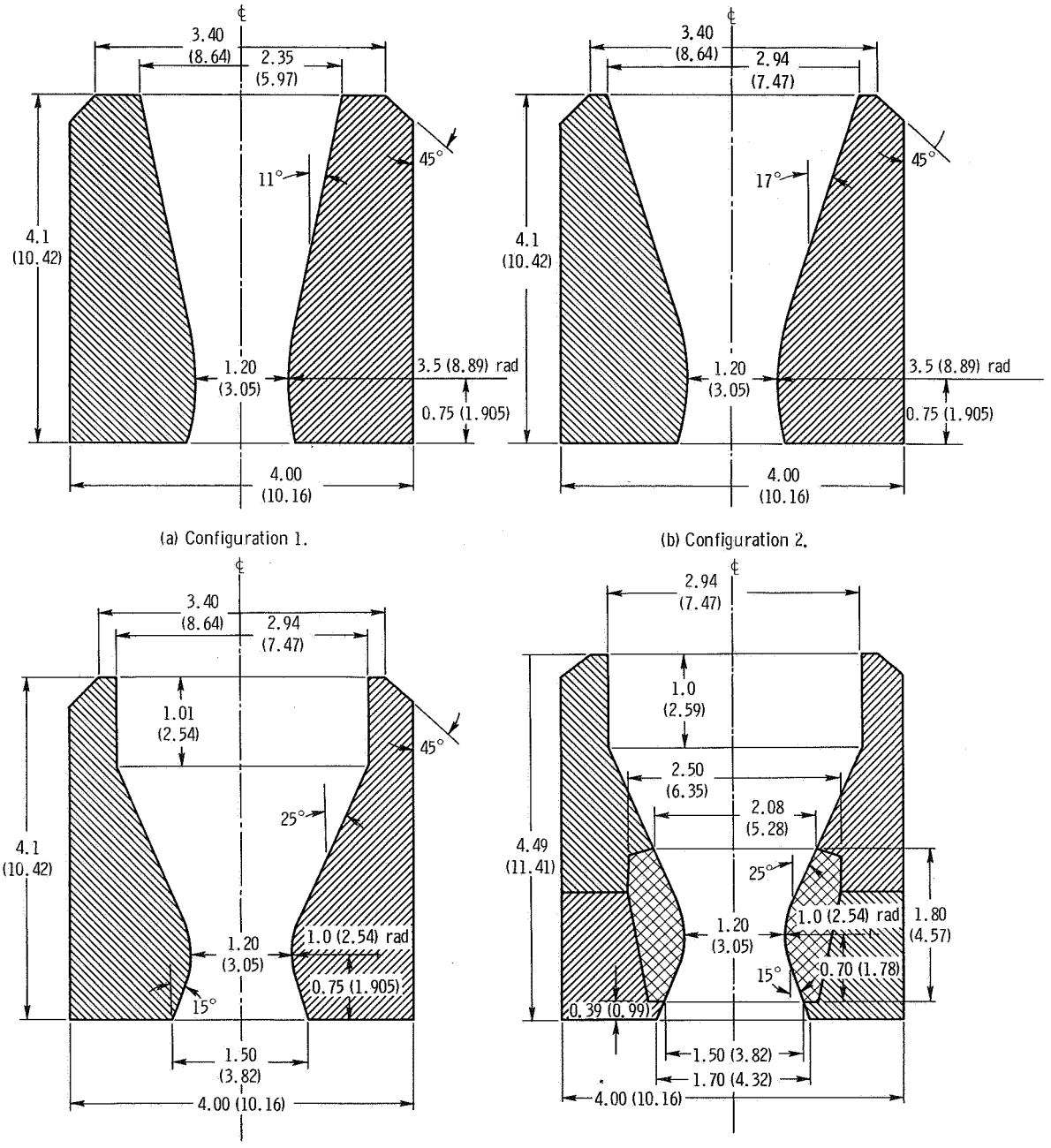

(a) Configuration 1.

(b) Configuration 2.

(c) Configuration 3.

(d) Configuration 4.

Figure 5. - Nozzle configuration. (All linear dimensions are in inches (cm).)

except that the throat material was in the form of an insert. This configuration was used to test relatively expensive throat materials mounted in less costly holder materials.

Twenty two nozzles were fabricated out of 18 different ablative materials as listed in table I. Three different reinforcement materials were used: quartz, silica, and carbon-silica. The reinforcement was oriented in one of three ways: Fabric at 90° to the centerline, fabric at 60° to the centerline, and randomly oriented, chopped fabric squares 1/2 by 1/2 inch (1.27 by 1.27 cm). The five different resins used in these materials were phenolic, polyimide, phenolic plus polyamide, epoxy-novalac, and phenyl-silane.

The test stand shown in figures 1 and 2 was equipped to measure engine thrust with a strain-gage bridge type of load-cell that was loaded in tension by the weight of the engine and preload weights to slightly greater than the thrust of the engine, (nominally 140 lb (622 N)). When the engine was fired, the thrust partially relieved the tension force on the load cell, and the change in this tension force was recorded as measured thrust. The thrust measuring system was calibrated at regular intervals by systematically removing the preload weights to simulate engine thrust. The static pressure on the base of the engine exhaust nozzle was measured for each firing and was found to be approximately 0.2 psi (1.38 kN/m^2) less than atmospheric. The measured thrust was then corrected for this pressure-times-area term.

Chamber pressure was measured by two strain-gage bridge-type pressure transducers through the P_c tap in the injector face (figs. 3 and 4). At regular intervals, chamber pressure was also measured by a high frequency-response, piezoelectric transducer which was mounted through the wall and flush with the inner surface of one of the cylindrical water-cooled spool pieces. This was done to ascertain the absence of combustion instability.

Each of the propellant's flow was measured by two flowmeters in series: a turbine flowmeter and a Venturi flowmeter. They were calibrated together with water flow in a weigh tank facility. The calibrations were then adjusted for propellant densities. The fuel flows, as measured by the two flowmeters, agreed to within 1/2 percent. The oxidant flows differed by 4 percent. As a consequence of this discrepancy, an average of the two flowmeter readings was used in this test program. Propellant temperature was measured with iron-constantan and copper-constantan thermocouples referenced to a calibrated oven at 150° F (339° K).

All data were digitized and recorded at high speed on a magnetic tape for computation in a digital computer. Some pertinent parameters were displayed on recording oscillographs for onsite monitoring.

TABLE I. - LIST OF NOZZLES TESTED AND RESULTS

Nozzle	Configuration	Mixture ratio, O/F	Supplier	Supplier number	Reinforcement			Resin		Additive		1	2	3	4		5	
					Orientation to centerline, deg	Material	Weight percent	Material	Weight percent	Material	Weight percent	Duration in seconds to specified erosion calculated by flow		Total firing duration in seconds	Postfire erosion measurements by shadowgraph		Final erosion calculated by flow	
												80 mils (0.203 cm)	160 mils (0.406 cm)		mil	mm	mil	mm
1	1	1.68	U.S. Polymeric	FM5091	90	Quartz	70	Phenolic USP-39	30	---------	--	60	90	123	199	5.05	188	4.78
2	1	1.68	U.S. Polymeric	FM5324	90	Quartz	70	Phenolic F-505	30	---------	--	60	84	121	206	5.23	194	4.93
3	4	1.62	Avco	X6000C	90	Quartz	69	Polyimide	31	---------	--	47	77	96	208	5.28	198	5.03
4	1	1.64	Hitco	C-1554-48	90	Silica	71	Phenolic and polyamide	27	Chrome salts	2	44	69	95	208	5.28	217	5.51
5	1	1.68	U.S. Polymeric	FM5131	90	Silica	65	Phenolic	32	Pearlite	3	42	62	85	204	5.18	190	4.83
6	4	1.59	Avco	X2001	90	Silica and proprietary resin charred	92	Epoxy novalac	8	---------	--	39	68	89	202	5.13	204	5.18
7	1	1.64	Fiberite	MX2641	90	Silica	70	Phenolic R-113	30	---------	--	39	62	84	210	5.33	217	5.51
8	1	1.65	Fiberite	MXS115	90	Silica	70	Phenolic FR-1225	30	---------	--	38	58	77	220	5.59	210	5.33
9	1	1.64	U.S. Polymeric	FM5131	90	Silica	65	Phenolic	32	Pearlite	3	37	58	75	195	4.95	204	5.18

10	1	1.65	U.S. Polymeric	X2004	90	Quartz	59	Phenyl-silane	14	Elastomer	27	37	53	71	213	5.41	218	5.54
11	4	1.64	Avco	X6000	90	Silica	72	Phenolic	28	---	--	37	59	80	200	5.08	222	5.64
12	4	1.64	Avco	X6000B	90	Silica	70	Polyimide Skybond 700	30	---	--	32	59	88	200	5.08	200	5.08
13	4	1.61	Avco	X6000A	90	Silica	72	Polyimide PI 3301	28	---	--	31	60	72	205	5.21	206	5.23
14	1	1.67	U.S. Polymeric	XR2015	60	Silica	62	Phenyl-silane	13	Elastomer	25	28	44	65	210	5.33	200	5.08
15	4	1.63	Avco	X2001	90	Silica and proprietary resin charred	83	Epoxy novalac	17	---	--	26	41	54	192	4.88	195	4.95
16	1	1.99	Fiberite	MXSC195	1/2×1/2	Carbonsilica	60	Phenolic	40	---	--	28	37	46	196	4.97	198	4.83
17	1	2.06	Fiberite	MX2641	90	Silica	70	Phenolic	30	---	--	44	68	92	212	5.38	220	5.59
18	3	2.03	Haveg	Planeton IV-2	90	Silica	80	Phenolic and polyamide	20	---	--	42	68	95	234	5.94	240	6.10
19	2	2.03	Haveg	Planeton IV-2	90	Silica	80	Phenolic and polyamide	20	---	--	40	67	98	244	6.20	248	6.30
20	1	2.07	Haveg	Planeton IV-2	90	Silica	80	Phenolic and polyamide	20	---	--	40	65	97	216	5.49	254	6.45
21	1	2.01	Haveg	Planeton IV-1	1/2×1/2	Silica	64	Phenolic	30	Ceramic frit	6	40	64	95	237	6.02	250	6.35
22	1	2.01	Haveg	Planeton IV-1	1/2×1/2	Silica	64	Phenolic	30	Ceramic frit	6	36	55	102	269	6.83	261	6.63

PROCEDURE

Each test nozzle was fired only once to maximum throat erosion while P_c and O/F were held constant. To maintain a constant chamber pressure, the propellant flow was increased by the controller as required. The propellant flow is related to the throat area by the relation

$$\Delta W = \frac{P_c \, g \, \Delta A_T}{C^*} \tag{1}$$

When P_c, g, and C* are constant,

$$\Delta W \propto \Delta A_T \tag{2}$$

where ΔW is the change in the propellant weight flow, g is a constant equal to 32.179 feet per second squared (9.80 m/sec^2), ΔA_T is the change in throat area, and C* is the characteristic exhaust velocity. The maximum radial throat erosion (limited by the propellant flow capacity) was approximately 200 mils (0.58 cm) for O/F = 1.6 and approximately 250 mils (0.635 cm) for O/F = 2.0.

Periodically during the course of the program, several heat-sink copper nozzles of throat measurements ranging from 1.2 to 1.7 inches (3.05 to 4.32 cm) were fired for short duration (6 sec) to determine (or calibrate) C* and its variation as a function of O/F and A_T, and to ascertain that it was constant.

From these known or calibrated values of C* and from measured values of propellant flow and chamber pressure, the effective throat area of each ablative nozzle was calculated as a function of firing time. The area was then converted to an effective throat radius, and the erosion value was calculated. A postfire check of each ablative nozzle consisted of tracing an outline of the throat as projected by a 10 power optical comparator (shadowgraph), and then measuring the area on the paper with a planimeter to determine A_T. This procedure yielded an independent value of throat erosion. In most cases, the erosion calculated by the two methods agreed to ±0.014 inch (0.0256 cm).

RESULTS AND DISCUSSION

Combustion Performance

The variation of erosion rate of ablative materials with small changes in combustion performance is very significant (unpublished data). Before comparisons between ablative

materials are valid, it must be established that combustion performance is constant. The characteristic-exhaust-velocity efficiency was therefore determined from firings of the heat-sink nozzles before, during, and after the ablative test program to monitor combustion performance and to ascertain that it did not vary during the program. Characteristic-exhaust-velocity efficiency ηC^* was calculated two different ways

$$\eta C^* = \frac{F}{W I_{sp,th}} \eta C_f \tag{3}$$

$$\eta C^* = \frac{P_c A_T g}{W C^*_{th}} \tag{4}$$

where F is the corrected thrust (measured thrust plus the base force), $I_{sp,th}$ is the theoretical specific impulse, ηC_f is the thrust coefficient efficiency, and C^*_{th} is the theoretical characteristic exhaust velocity. The C^* efficiency as calculated by the first method (eq. (3)) was 95.1±1.3 percent at $O/F = 1.6$ and 95.9±0.8 percent at $O/F = 2.0$. All the data fell within these limits, yielding a standard deviation of ±1.5 percent. These values of ηC^* were substantiated to within ±0.5 percent by the second method (eq. (4)), when a ηC_f value of 95.5 was used. This value of ηC_f is less than the values used for large contoured nozzles with the same radius of curvature to radius of throat ratio (0.5). But the value of ηC_f could be justified because of the small nozzle diameter, which magnified the effect of boundary-layer displacement thickness and momentum deficiency.

General Erosion Characteristics

Uniformity of the injector pattern is indicated in figure 6, which is an axial view of the throat plane of a typical sectioned nozzle after firing. The circle in the center shows the original throat profile. The erosion, though not entirely symmetrical, was free of major gouges and streaks, and the char layer was of uniform thickness. The firing duration of 95 seconds and erosion of approximately 237 mils (0.602 cm) still left a considerable amount of uncharred virgin material.

A typical erosion history is shown in figure 7 which is a curve faired through many points of calculated throat radius change (by propellant flow) as a function of firing duration (for nozzle 21). The initial throat radius change is in a negative direction at the start of the firing. This phenomena occurs during the time it takes surface erosion at the throat to start, and can be caused by one or a combination of effects: (1) a thickening of the boundary layer by volatile outgassing and/or surface roughening, (2) a swelling of the wall material caused by thermal expansion and/or charring, (3) flow of molten upstream

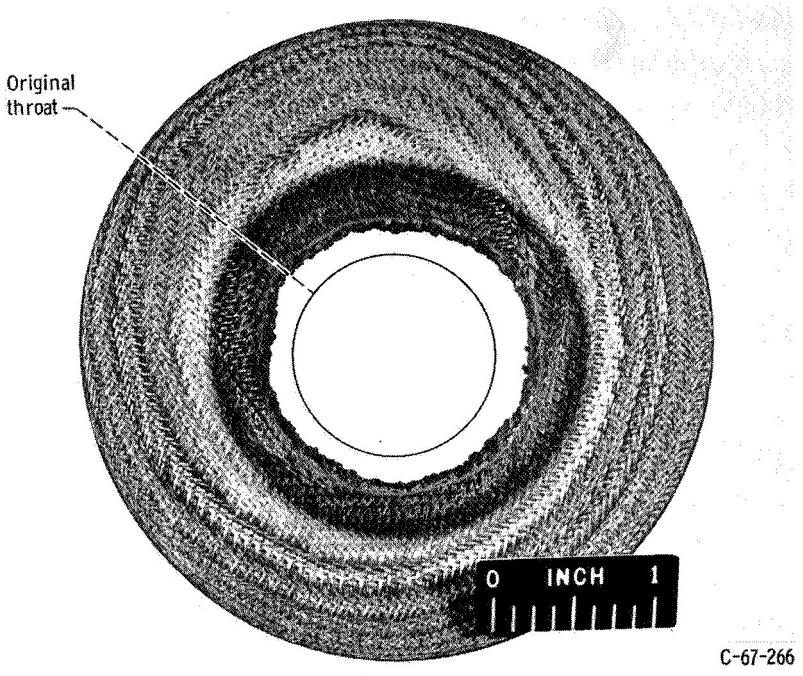

Figure 6. - Postfire photograph of typical nozzle sectioned at throat plane. Nozzle 18.

material over the throat. The magnitude of this negative erosion phenomena and its duration were very similar for all ablative nozzles discussed in this report. The negative erosion phenomena of reference 3 however, seemed to be caused primarily by volatile outgassing, and was significantly affected by resin content of the ablative material.

Also shown in figure 7 are four of the values tabulated in the last five columns of table I. The circled points are the erosion values calculated from flow just before the end of the firing and at 80 and 160 mils (0.203 and 0.406 cm) erosion. The square symbol shows the value of erosion calculated from postfire shadowgraph measurements. In most cases, the shadowgraph measurements agreed with the erosion calculated from flow at the end of the firing to within ±0.014 inch (0.0256 cm), as shown in the last two columns of table I (Columns 4 and 5).

Figure 8 contains the results presented in table I in a generalized form to show the relative erosion resistance of the 22 nozzles tested. Values plotted are expressed as percent of the firing duration achieved using the best nozzle (nozzle 1). Three values calculated from flow are shown for each nozzle to compare the relative erosion resistance of the nozzles at three durations. A fourth value calculated by postfire measurement illustrates the magnitude of data scatter and the degree of discrimination possible between nozzles. The length of the top bar for each nozzle is used to show the percent

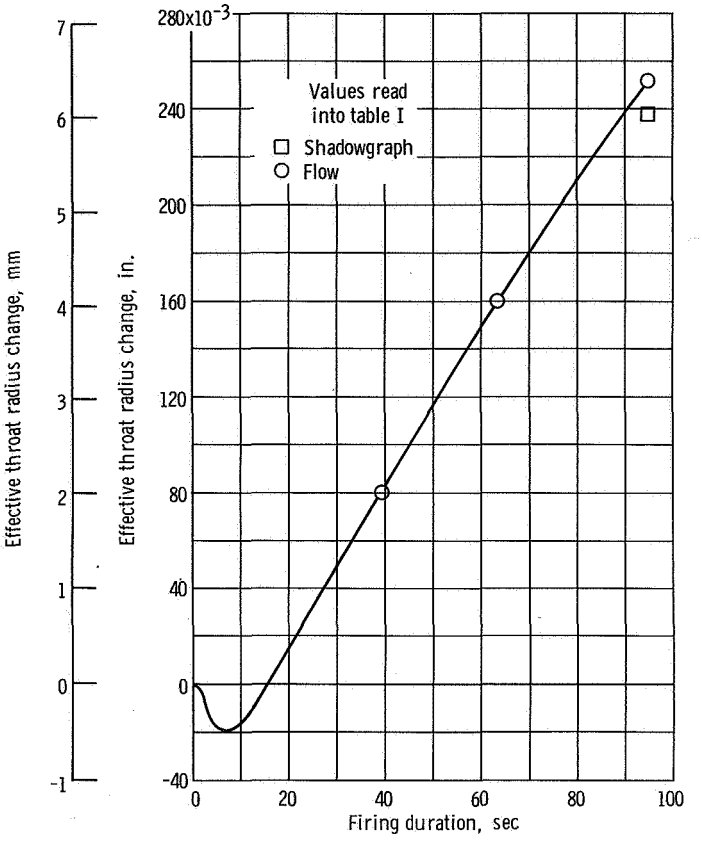

Figure 7. - Typical erosion history. Nozzle 21.

duration to a radial erosion of 80 mils (0.203 cm), as calculated from propellant flow. The best nozzle duration to 80 mils erosion was 60 seconds (nozzle 1, column 1, table I) and defines the absolute value of 100 percent for the first bar. The duration it took other nozzles to reach 80 mils erosion is then expressed in percent of 60 seconds.

The second bar for each nozzle similarly shows the percent duration, but to a radial erosion of 160 mils. From column 2 of table I, nozzle 1 took 90 seconds to reach a radial erosion of 160 mils (0.406 cm). The duration it took other nozzles to reach 160 mils erosion is then expressed in percent of 90 seconds.

The third bar for each nozzle shows the percent duration per mil of total radial erosion as calculated from postfire measurements by shadowgraph.

The fourth bar for each nozzle similarly shows the percent duration per mil of total radial erosion, but calculated from propellant flow.

It is apparent that ranking the nozzles according to the relative erosion resistance is the same regardless of the firing duration at which the comparison is made or the method

Figure 8. - Relative erosion resistance of ablative nozzles.

of measuring the erosion. Therefore, for comparisons of one ablative nozzle with another, an average of the four bars will be used.

Before discussing comparisons of the individual ablative nozzle variables, a determination of test result uncertainty is in order. This is seen by comparing the erosion performance of nozzles 21 and 22. These nozzles were supplied by the same supplier, of identical material, configuration and lot number, and fired under identical conditions. Nozzle 21 was fired near the beginning of the test program, whereas nozzle 22 was one of the last nozzles tested. Ideally, their erosion performance should have been identical. In reality, their erosion was different by $4\frac{1}{2}$ percent (by averaging 4 bars of each nozzle from fig. 8). This variation then sets the ground rules for all further comparisons of materials in this report and establishes the resolution to effects greater than $4\frac{1}{2}$ percent.

Effects of Specific Variables

A photograph showing the typical postfire appearance of two configurations (nozzles 4 and 15) is shown in figure 9. This is a view after sectioning and shows similarity in the char layers regardless of entrance angle. Nozzles 18 to 20 were used to investigate the effect of convergent entrance angle and nozzle throat radius of curvature on erosion rate. Not only did nozzle configuration have no effect on char layer, it had no effect on erosion rate (fig. 10(a)).

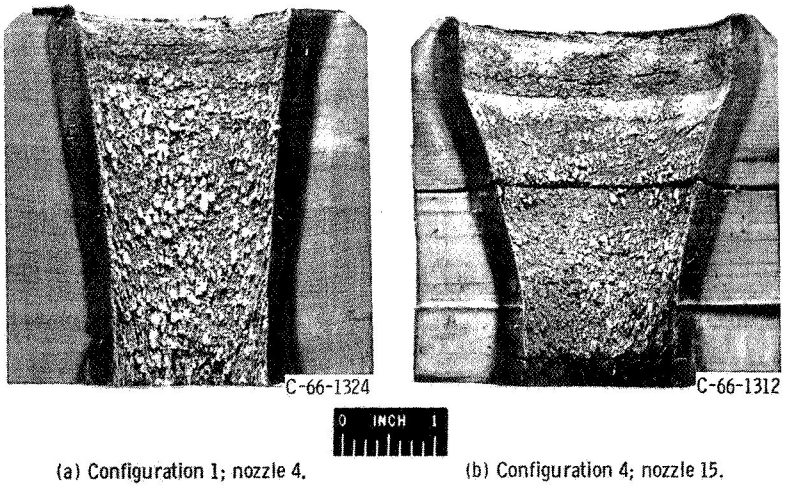

(a) Configuration 1; nozzle 4. (b) Configuration 4; nozzle 15.

Figure 9. - Typical eroded test nozzles after sectioning.

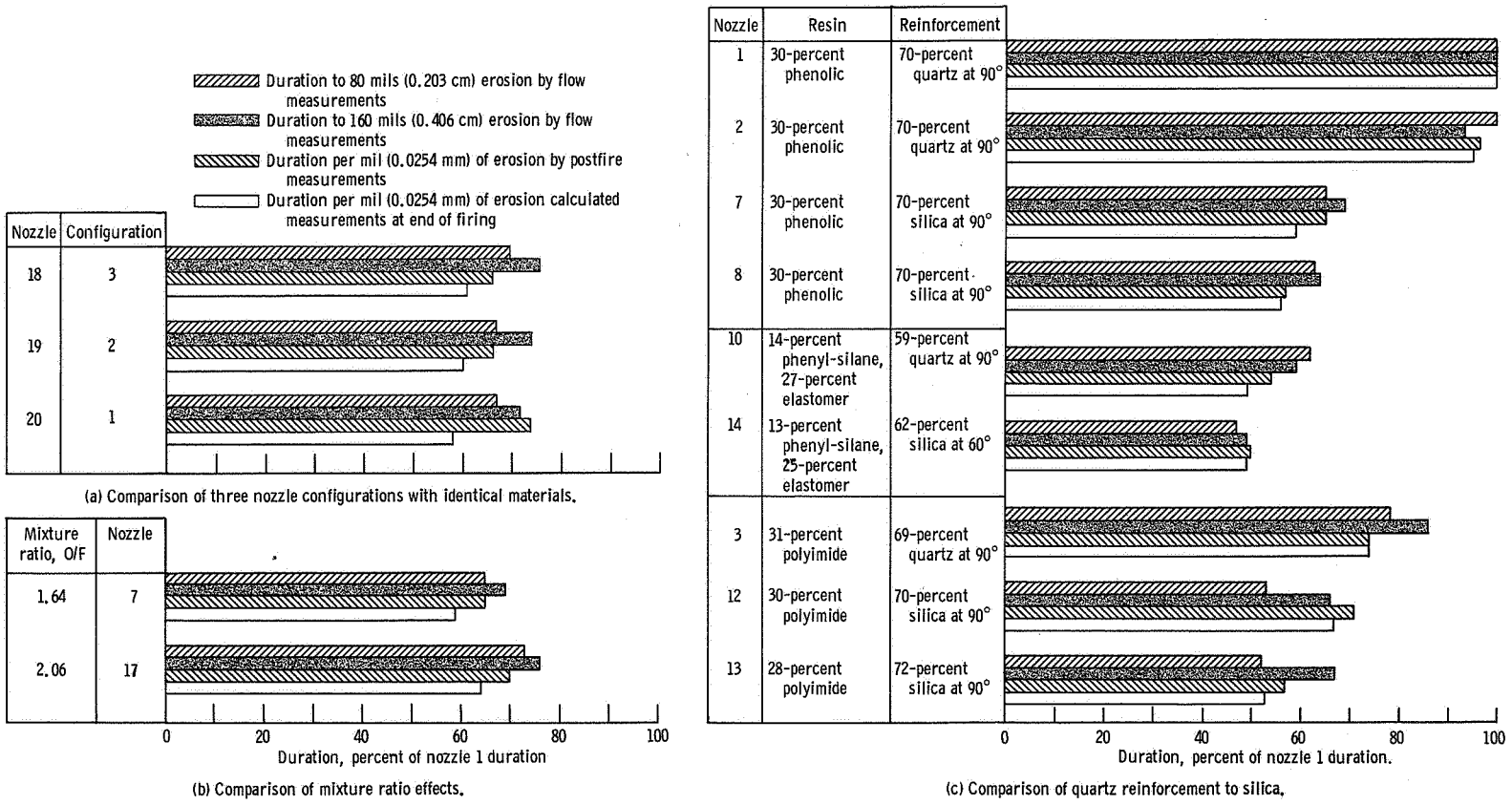

(a) Comparison of three nozzle configurations with identical materials.

(b) Comparison of mixture ratio effects.

(c) Comparison of quartz reinforcement to silica.

Figure 10. - Relative erosion resistance of ablative nozzles. (See table I for complete description of nozzles.)

Recent storable-propellant stage development is being directed at O/F = 1.6. Previous work (refs. 1 and 3) was done at O/F ratios of 2.0. To determine whether the O/F ratio change from 2.0 to 1.6 has any appreciable effect on erosion of ablative nozzles, two firings were performed on identical nozzles (7 and 17) at the two mixture ratios. Nozzle 7 was fired at O/F = 1.64 and nozzle 17 was fired at an O/F = 2.06. It was expected that the erosion at O/F = 1.64 would be less than the erosion at O/F = 2.06 because of the lower theoretical temperature and because of less oxygen in the exhaust products to oxidize the carbonaceous char. The test results (see fig. 10(b)) showed, however, that the erosion was slightly greater at O/F = 1.64 yielding about $6\frac{1}{4}$ percent less duration to the same total erosion as O/F = 2.04.

Although quartz and silica are both silicon dioxide (SiO_2), quartz was the better ablative reinforcement material. The difference between silica and quartz is only purity. Silica is defined as approximately 99.0 percent silicon dioxide, whereas quartz is defined as approximately 99.6 percent silicon dioxide. Impurities tend to form eutectic mixtures with silicon dioxide and result in lower melting temperatures. Impurities also tend to decrease the viscosity of the melted silicon dioxide and make it flow more easily. Both these mechanisms should contribute to make silica less erosion resistant than quartz. The advantage of using quartz instead of silica as a reinforcement material is shown for three resin systems in figure 10(c). Nozzles 1, 2, 7, and 8 show the comparison when using a phenolic resin, nozzles 10 and 14 for phenyl-silane resin with elastomer additive, and nozzles 3, 12, and 13 for polyimide resin. In all cases, the quartz reinforcement was better. The quartz reinforcement increased nozzle duration over 30 percent for phenolic and 6 percent for phenyl-silane with elastomer. It is also apparent that, with better resin systems, quartz makes more of an improvement than with poorer resin systems.

The effect of using phenolic resin instead of polyimide resin is shown in figure 10(d) for two reinforcements. Results with nozzles 1, 2, and 3 are given to show the effect with quartz reinforcement, and results with nozzles 8, 11, 12, and 13 to show the effect with silica reinforcements. The phenolic resin is clearly the superior resin when used with quartz reinforcement. With silica reinforcement, there was no improvement within the magnitude of the experimental uncertainty ($4\frac{1}{2}$ percent).

To determine whether slight variations in fabrication technique would have any effect on the erosion resistance of ablative materials, the same material (FM 5131 from U.S. Polymeric) was specified for nozzles from two different fabricators. These ablative nozzles (5 and 9) were test fired, and the results are shown in figure 10(e). Nozzle 5 had a duration $7\frac{1}{2}$ percent longer than nozzle 9, indicating a slight effect of fabrication technique. Therefore, to achieve a materials full potential, a determination of the effects of several fabrication variables on erosion rate will be required along with careful control of the important variables during the fabrication process.

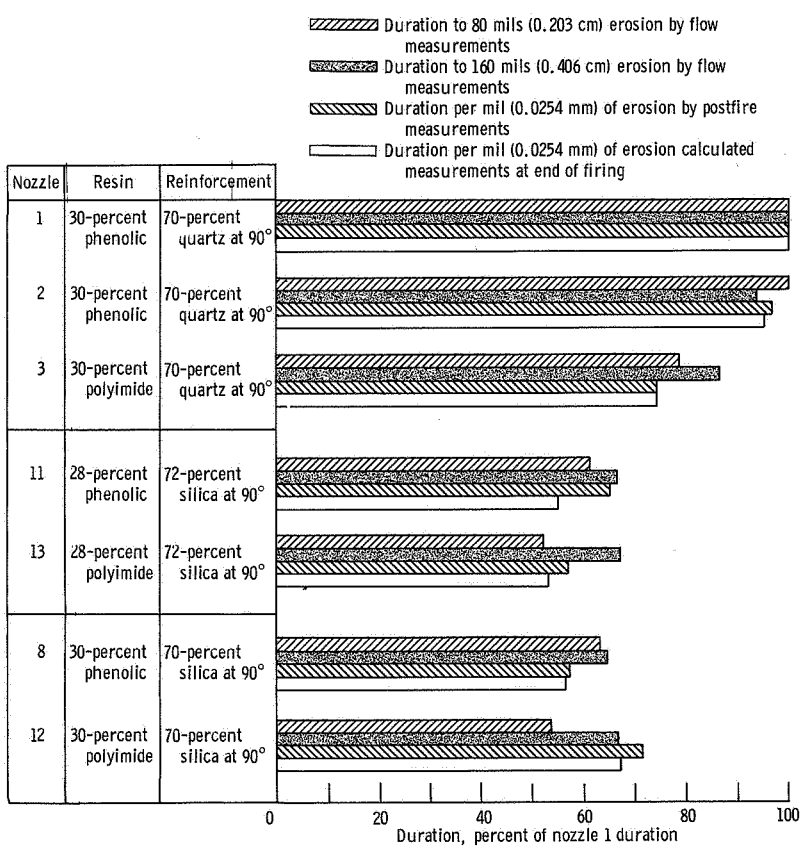

(d) Comparison of resin systems.

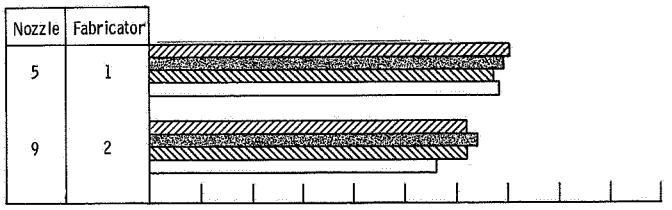

(e) Effect of fabrication technique.

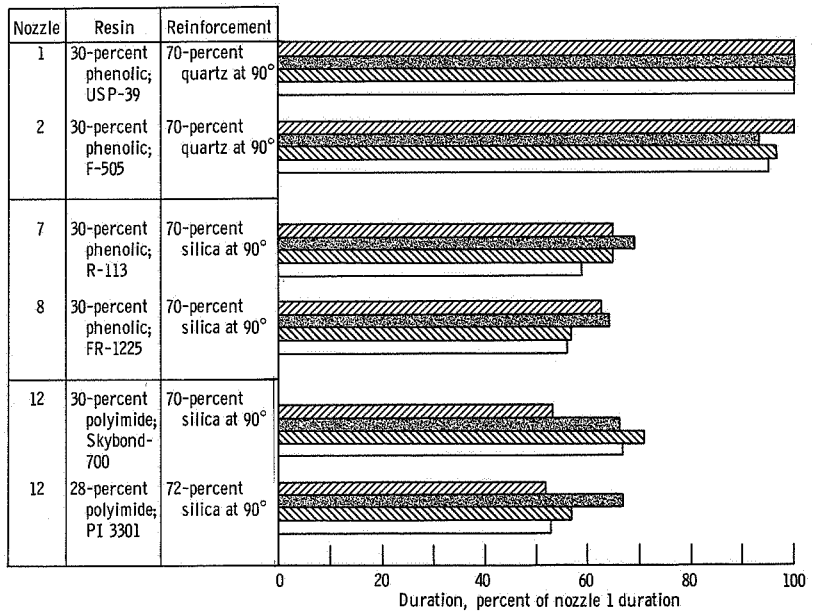

(f) Effect of different resin sources.

Figure 10. - Continued.

There are several different resins that comply to the typical resin specifications. Four phenolic resins, from different sources but manufactured to identical specifications, were evaluated (as well as two polyimide resins) to determine whether small variations in composition or manufacture (within the specifications) had any effect on erosion resistance. Figure 10(f) shows that resins obtained from various sources had equivalent erosion resistance. Phenolic resin USP-39 performed the same as phenolic resin F-505; phenolic resins R-113 and FR-1225 were similar; and polyimide resins Skybond 700 and PI 3301 were also similar. Unlike fabrication specifications, it is apparent that resin specifications are adequate, and the small differences among the resins tested herein had no effect on nozzle erosion resistance.

Attempts to improve the erosion resistance of some ablatives have been made by precharring the material in an oven and then reimpregnating the charred material with resin. The initial charring process causes the formation of silicon carbide and graphites which are intended to reduce the erosion in some environments. To determine whether this process has any advantage in the storable-propellant environment, two nozzles were precharred and then reimpregnated with resin. (Nozzles 6 and 15). Initial fabrication used silica cloth reinforcement and a proprietary resin. Nozzle 6 was a high-pressure molded prepreg, which is silica cloth preimpregnated with uncured resin compressed into billet shape at high pressures and then cured. Nozzle 15 was the same reinforcement and resin, but it was low-pressure vacuum impregnated and then cured. Because of the lower pressure involved, nozzle 15 was less dense than nozzle 6. At this point in the fabrication, both nozzles were oven-charred, and then reimpregnated with epoxy-novalac resin. Since nozzle 6 was more dense, it took on less of the epoxy-novalac resin than nozzle 15 (8 percent for 6 and 17 percent for 15). The increased density of nozzle 6 may also have contributed to its better erosion resistance, as is shown in figure 10(g). Oven charring and reimpregnating seem to show no advantage over conventionally processed ablatives in the storable-propellant combustion environment. The reason appears to be that any refractories formed (silicon carbide and graphite) are very prone to oxidation in this environment.

Chrome salt was added to silica reinforcement (ref. 3) to enhance the silica viscosity, slowdown its flow, and thereby improve the erosion resistance of the ablative material. Nozzle 4 had 2 percent of this chrome salt, whereas nozzle 18 had none. The relative erosion resistance of these two nozzles (shown in fig. 10(h)) showed a slightly longer duration for nozzle 4, which indicates a possible advantage in adding the chrome salt. This effect, however, was within the experimental resolution previously discussed ($4\frac{1}{2}$ percent), and somewhat obscured by different resin reinforcement concentrations.

Previous testing (ref. 1) has shown that ablative materials made of graphite or carbon reinforcement have very poor erosion resistance in storable propellant environments because of their high susceptibility to oxidation. However, a recent development

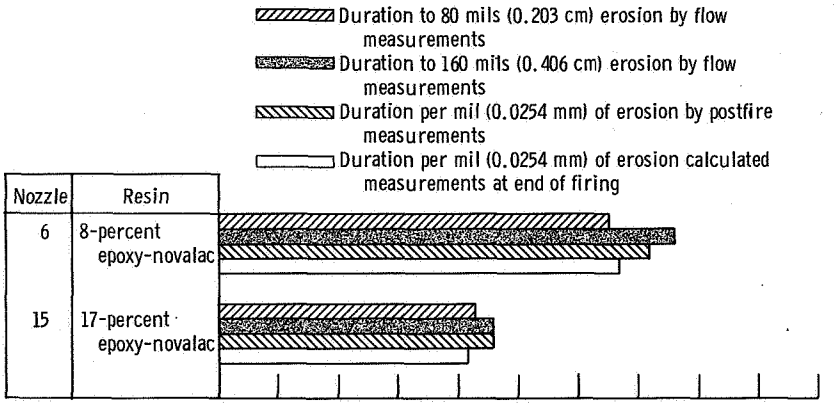

(g) Precharred and reimpregnated materials.

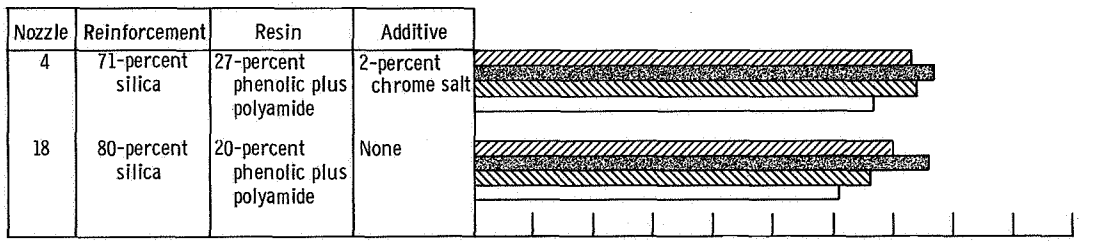

(h) Effect of chrome salt additive.

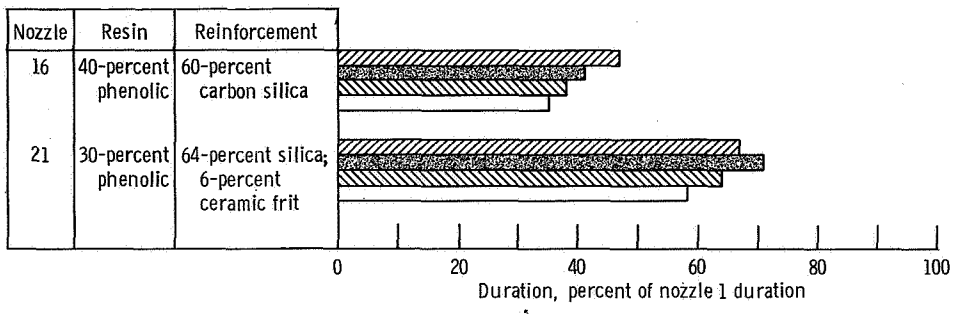

(i) Effect of carbon silica as reinforcement.

Figure 10. - Concluded.

in reinforcement material has produced carbon-silica fibers in which both materials exist as continuous filaments in each fiber. It was hoped that the presence of carbon would offer some structural strength when the silica started melting, and that the silica would offer some protection from oxidation to the carbon. A cloth woven of these fibers was used as a reinforcement material in nozzle 16. Figure 10(i) shows a comparison of the erosion resistance of two materials, one with carbon-silica reinforcement and one with silica reinforcement. The silica reinforcement was better than the carbon-silica reinforcement by a 25-percent longer duation. The lesser amount of resin in the silica material may have contributed somewhat to its increased duration; however, the primary effect is probably because of superior reinforcement. Apparently, the high-temperature resistance of the carbon was more than compromised by the susceptibility of the carbon to oxidation in this environment.

SUMMARY OF RESULTS

Twenty-two ablative nozzles were fired at 1.2-inch (3.05-cm) diameter throat sections for a storable-propellant (nitrogen tetroxide and a 50-50 percent blend of unsymmetrical dimethylhydrazine with anhydrous hydrazine) rocket engine at a chamber pressure of 100 psia (689.5 kN/m^2), mixture ratios of 1.6 and 2.0, and a characteristic-exhaust-velocity efficiency of approximately 95.5 percent. Resolution of the erosion tests were within $4\frac{1}{2}$ percent and are summarized as follows:

(1) Quartz was a better reinforcement with the three resins tested than silica. The superiority is attributed to the higher melting temperature of quartz.

(2) Phenolic resin was superior to polyimide resin with quartz reinforcement. The two resins were equivalent when used with silica reinforcement.

(3) A mixture ratio of 1.6 was slightly more erosive than a mixture ratio of 2.0.

(4) A chrome-salt additive to the silica reinforcement produced only slight improvement.

(5) Silica-carbon reinforcement was relatively poor because of the rapid oxidation of the carbon.

(6) Fabrication technique had a slight effect on erosion resistance.

(7) Different resins of identical specifications but from different suppliers performed equally well.

(8) Nozzle convergent entrance angle and throat radius of curvature had no effect on erosion resistance.

Lewis Research Center,
National Aeronautics and Space Administration,
Cleveland, Ohio, October 31, 1967,
128-31-03-00-22.

REFERENCES

1. Peterson, Donald A.; and Meyer, Carl L.: Experimental Evaluation of Several Ablative Materials as Nozzle Sections of a Storable-Propellant Rocket Engine. NASA TM X-1223, 1966.

2. Salmi, Reino J.; Wong, Alfred; and Rollbuhler, Ralph J.: Experimental Evaluation of Various Nonmetallic Ablative Materials as Nozzle Sections of Hydrogen-Oxygen Rocket Engine. NASA TN D-3258, 1966.

3. Peterson, Donald A.: Experimental Evaluation of High-Purity-Silica Reinforced Ablative Composites as Nozzle Sections of 7.8-Inch- (19.8-cm) Diameter Throat Storable-Propellant Rocket Engine. NASA TM X-1391, 1967.

4. Shinn, Arthur, M., Jr.: Experimental Evaluation of Six Ablative-Material Thrust Chambers as Components of Storable-Propellant Rocket Engines. NASA TN D-3945, 1967.

5. Rowley, R. W.: An Experimental Investigation of Uncooled Thrust Chamber Materials for Use in Storable Liquid Propellant Rocket Engines. Tech. Rep. No. 32-561 (NASA CR-53367), Jet Propulsion Lab., California Inst. Tech., Feb. 15, 1964.

6. Anon.: AVCO Pre-Char Rocket Nozzle Materials. Rep. No. AVSSD-0101-67-RM, AVCO Corp., 1967.

NASA-Langley, 1968 — 28 E-4171